# Design of wind farm layout for maximum wind energy capture

Andrew Kusiak*, Zhe Song

*Intelligent Systems Laboratory, Mechanical and Industrial Engineering, 3131 Seamans Center, The University of Iowa, Iowa City, IA 52242 – 1527, USA*

ABSTRACT

Wind is one of the most promising sources of alternative energy. The construction of wind farms is destined to grow in the U.S., possibly twenty-fold by the year 2030. To maximize the wind energy capture, this paper presents a model for wind turbine placement based on the wind distribution. The model considers wake loss, which can be calculated based on wind turbine locations, and wind direction. Since the turbine layout design is a constrained optimization problem, for ease of solving it, the constraints are transformed into a second objective function. Then a multi-objective evolutionary strategy algorithm is developed to solve the transformed bi-criteria optimization problem, which maximizes the expected energy output, as well as minimizes the constraint violations. The presented model is illustrated with examples as well as an industrial application.

© 2009 Elsevier Ltd. All rights reserved.

## 1. Introduction

The wind energy market is rapidly expanding worldwide [1]. This rapid growth of the wind energy industry has led to cost reduction challenges. There are various ways of reducing the cost of producing wind power: for example, the site selection, site layout design, predictive maintenance, and optimal control system design [13]. The wind farm layout design is an important component of ensuring the profitability of a wind farm project. An inadequate wind farm layout design would lead to lower than expected wind power capture, increased maintenance costs, and so on. Equation (1) captures the cost of energy (*COE*) [12]

$$COE = \frac{C_I \times FCR + C_R}{AEP} + C_{O\&M} \tag{1}$$

where $C_I$ is the initial capital cost ($) of the wind farm; *FCR* is the fixed charge rate (%/year); $C_R$ is the levelized replacement cost ($/year); $C_{O\&M}$ is the cost of maintenance and operations ($/kWh); *AEP* is the annual energy production (kWh/year)

Note that at the design stage, *AEP* is the expected (planned) wind energy production. The annual energy production *AEP* is affected by the turbine availability, i.e., the number of operational hours in a year. Maximizing the *AEP* is an effective approach for reducing the cost of energy production. In this paper, *AEP* is improved by optimizing the wind farm layout design, specifically minimizing the wake loss.

Wind farm layout has been addressed in the literature [4,6,9,17]. Grady *et al.* [4] and Mosetti *et al.* [9] used a genetic algorithm to minimize a weighted sum of wind energy and turbine costs. The wind farm is divided into a square grid to facilitate the encoding of a 0–1 type solution. Lackner and Elkinton [6] presented a general framework to optimize the offshore wind turbine layout. Details of how to solve the optimization problem are neither discussed in ref. [6], nor any other wind farm layout design tools, such as WASP [18]. Castro Mora *et al.* [17] also used a genetic algorithm to maximize an economic function, which is related to turbine parameters and locations. Similarly in ref. [17], the wind farm is represented with a square grid. One of the shortcomings of the approach presented in [17] was that wake loss was not considered. In ref. [4,9], the wind energy calculation is not based on the power curve function, and wind direction was not fully discussed in their optimization models. This paper extends the approach of [6] by developing specific mathematical models to calculate the wake loss based on turbine locations. Solution of the constrained optimization problem is fully discussed with a double-objective evolutionary strategy algorithm, which can be easily extended by considering additional constraints.

## 2. Problem formulation and methodology

Modeling the wind farm layout design problem calls for assumptions. However, the assumptions made in this paper are acceptable in industrial applications and they could be modified or even removed, if necessary.

**Assumption 1**. For a wind farm project, the number of wind turbines *N* is fixed and known before the farm is constructed.
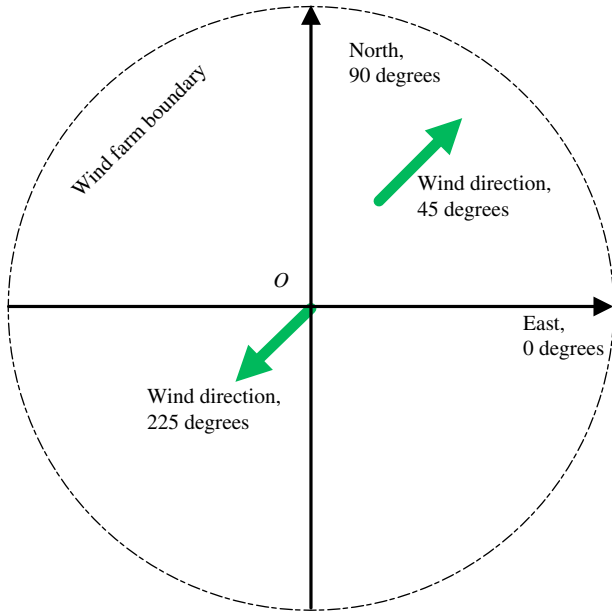
**Fig. 1.** Wind farm boundary and the definition of the wind speed direction.

A typical wind farm project has its total capacity goal dictated by various factors, e.g., finances and turbine availability. For example, to achieve 150 MW (Mega Watt) capacity, a hundred 1.5 MW turbines are needed.

**Assumption 2**. Wind turbine location is characterized by its two-dimensional Cartesian coordinates $(x,y)$, represented as a vector $\boldsymbol{x}$ of the length $\sqrt{x^2 + y^2}$. This assumption implies that the terrain has relatively small variations of surface roughness. The optimal solution computed in this paper is represented by $N$ Cartesian coordinates $(x_i, y_i)$, $i = 1,\ldots,N$.

**Assumption 3**. The wind turbines considered for a wind farm are homogenous, i.e., they all have the same power curve function $P = f(v)$, where $v$ is the wind speed at the wind turbine rotor with a fixed height, $P$ is the turbine power output. The wind turbine nacelle is usually controlled so that the rotor is oriented perpendicularly to the wind direction. For ease of turbine operations and maintenance, wind farm developers usually deal with one supplier of wind turbines delivering one turbine type.

**Assumption 4**. Wind speed $v$ (at a given location, height, and direction) follows a Weibull distribution $p_v(v, k, c) = k/c(v/c)^{k-1}e^{-(v/c)^k}$, where $k$ is the shape parameter, $c$ is the scale parameter, and $p_v(.)$ is the probability density function. Note that Assumption 4 may not hold for short-time horizons; however, a great number of sites have shown Weibull distribution of the wind speed [8].

**Assumption 5**. At a given height, wind speed (a parameter of the Weibull distribution function) $v$ is a continuous function of the wind direction $\theta$, i.e., $k = k(\theta)$, $c = c(\theta)$, $0 \leq \theta \leq 360$. In other words, wind speeds at different locations with the same direction share the same Weibull distribution across a wind farm. The parameter $\theta$ is also assumed to have a continuous probability distribution $p_\theta(\theta)$.

In a relatively flat terrain, Assumption 5 is a reasonable one. Moreover, if the wind farm does not cover a wide range of terrain, the wind speeds at a fixed direction should share a similar distribution. Future research could consider the wind speed distributions changing with directions and locations.

Wind direction is an important parameter in this paper. Fig. 1 illustrates wind direction for a wind farm, where North is defined as $90°$ and East is defined as $0°$. Though wind turbines may follow

different layout patterns, here it is assumed that all turbines are placed within a circular boundary of a wind farm.

**Assumption 6**. Any two turbines in a wind farm are separated from each other by at least 4 rotor diameters.

Ensuring sufficient spacing between adjacent turbines reduces interactions, e.g., wind turbulence, thus diminishing the hazardous loads on the turbine. Given the rotor radius $R$, any two wind turbines located at $(x_i, y_i)$ and $(x_j, y_j)$ should satisfy the inequality $(x_i - x_j)^2 + (y_i - y_j)^2 \geq 64 R^2$.

Assumption 6 is based on certain domain heuristics [8]. However, it can be replaced by more complex constraints. For example, the minimum distance between two turbines can be a function of the wind direction and its probability.

For a single wind turbine located at $(x,y)$ and wind direction $\theta$, the expected energy production is

$$E(P, \theta) = \int_0^\infty f(v) p_v(v, k(\theta), c(\theta)) \mathrm{d}v$$
$$= \int_0^\infty f(v) \frac{k(\theta)}{c(\theta)} \left(\frac{v}{c(\theta)}\right)^{k(\theta)-1} e^{-(v/c(\theta))^{k(\theta)}} \mathrm{d}v \quad (2)$$

Integrating the expression in (2) for $\theta$ in the range 0–360 provides the expected energy production of a single wind turbine [6,8]

$$E(P) = \int_0^{360} p_\theta(\theta) E(P, \theta) \mathrm{d}\theta$$
$$= \int_0^{360} p_\theta(\theta) \mathrm{d}\theta \int_0^\infty f(v) \frac{k(\theta)}{c(\theta)} \left(\frac{v}{c(\theta)}\right)^{k(\theta)-1} e^{-(v/c(\theta))^{k(\theta)}} \mathrm{d}v \quad (3)$$

In this paper, optimizing $E(P)$ is considered equivalent to optimizing AEP as the number of operational hours is fixed. Note that in Equation (3), the wind speed is integrated from 0 to infinity, which is equivalent to integrating the wind speed from 0 to the cut-out speed. Once the wind speed is greater than the cut-out speed, a wind turbine is shut down for safety and it produces zero energy.

Model (4) represents an ideal scenario for maximizing the total wind energy captured by turbines, where the interactions among turbines are neglected, with $r$ being the radius of the wind farm. Note that the circular boundary of a wind farm can be easily modified to a rectangular boundary.

$$\max \sum_{i=1}^{N} E(P)$$
$$s.t. (x_i)^2 + (y_i)^2 \leq r^2, i = 1 \ldots N \quad (4)$$
$$(x_i - x_j)^2 + \left(y_i - y_j\right)^2 \geq 64R^2, i,j = 1 \ldots N, i \neq j$$

The major interactions among the turbines result in the energy loss caused by the wind turbine wakes. A wind farm design for the maximum of wind energy capture must minimize the wake effects among turbines.

### 2.1. The wake loss model

Wake loss is an important factor in considering wind park layout design [10]. When a uniform incoming wind encounters a wind turbine, a linearly expanding wake behind the turbine occurs [5,6]. A portion of the free stream wind's speed will be reduced from its original speed $v_{up}$ to $v_{down}$. Fig. 2 illustrates the basic concept of wake behind a wind turbine.
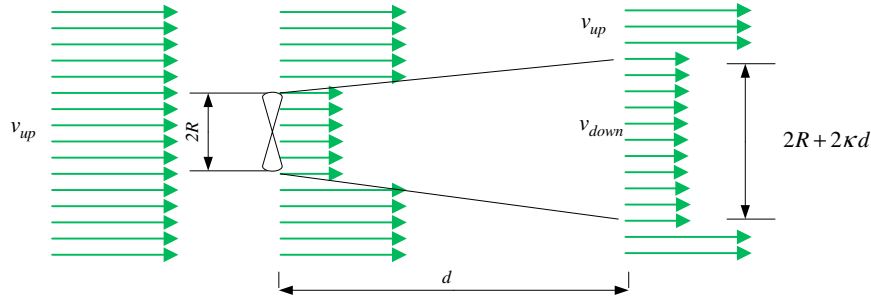
**Fig. 2.** Wind turbine wake model.

The velocity deficit is defined as the fractional reduction of free stream wind speed in the wake of the turbine, and it is calculated from equation (5).

$$Vel\_def = 1 - v_{\text{down}}/v_{\text{up}} = \left(1 - \sqrt{1 - C_{\text{T}}}\right)\bigg/(1 + \kappa d/R)^2 \qquad (5)$$

where $C_{\text{T}}$ is the thrust coefficient of the turbine; $\kappa$ is the wake spreading constant, and $d$ is the distance behind the upstream turbine following the wind direction.

Equation (5) can be simplified if $C_{\text{T}}$ and $\kappa$ are assumed to be constant for all turbines [6].

$$Vel\_def = 1 - v_{\text{down}}/v_{\text{up}} = \frac{a}{(1 + bd)^2} \qquad (6)$$

where $a = 1 - \sqrt{1 - C_{\text{T}}}$, $b = \kappa/R$.

For any two turbines' located at $(x_i, y_i)$ and $(x_j, y_j)$ in a wind farm, $Vel\_def_{i,j}$ is defined as the velocity deficit at turbine $i$ in the wake of turbine $j$. The wind direction is from $j$ to $i$, $d_{i,j}$ is the distance between turbine $j$ and $i$ projected on the wind direction $\theta$.

$$Vel\_def_{i,j} = \frac{a}{(1 + bd_{i,j})^2} \qquad (7)$$

When a turbine is affected by the wakes of multiple turbines, the total velocity deficit is computed as (8).

$$Vel\_def_i = \sqrt{\sum_{j=1, j \neq i}^{N} Vel\_def_{i,j}^2} \qquad (8)$$

where $Vel\_def_i$ is the total wind speed deficit at turbine $i$. However, for a given wind direction, not all turbines generate the wake effects at turbine site $i$.

Given wind direction $\theta$, all wind turbines' rotors are normally positioned perpendicular to the wind direction. The wake behind a turbine could be seen as a part of an imaginary cone. Fig. 3 illustrates a half cone formed by a turbine located at $(x, y)$ and the imaginary vertex $A$. Parameter $\alpha (0 \leq \alpha \leq \pi/2)$ is calculated as $\arctan(\kappa)$, and the distance between $A$ and the rotor center point is $R/\kappa$.

Fig. 4 shows 5 turbines in a wind farm. If wind blows from the West, turbine 2 is in the wake of turbine 1. Turbine 3 is in the wake

of turbine 1 and turbine 4. Turbine 5 is not affected by the wake of any other turbine.

**Lemma 1**. Given the wind direction $\theta$, any two wind turbines, $i$ and $j$ located within the wind farm, the angle $\beta_{i,j}$, $0 \leq \beta \leq \pi$, between the vector, originating at turbine $j$'s cone vertex $A$ to turbine $i$ and the vector, originating at $A$ to turbine $j$, $\beta_{i,j}$ is calculated as

$$\beta_{i,j} = \cos^{-1}\left\{\frac{(x_i - x_j)\cos\theta + \left(y_i - y_j\right)\sin\theta + R/\kappa}{\sqrt{\left(x_i - x_j + \frac{R}{\kappa}\cos\theta\right)^2 + \left(y_i - y_j + \frac{R}{\kappa}\sin\theta\right)^2}}\right\} \qquad (9)$$

Proof:

Consider wind direction $\theta$ in Fig. 5, origin $O$, and any two turbines $i$ and $j$ (without loss of generality, assume $i = 1, j = 2$) represented by vectors $\boldsymbol{x}_1$ and $\boldsymbol{x}_2$, located at $T1$ and $T2$, respectively. The vector $\overrightarrow{AT1}$ originating at $A$ to $T1$ (Turbine 1) should also have angle $\theta$, and its length is $L_{\overrightarrow{AT1}} = R/\kappa$. Vector $\overrightarrow{OA}$ can be expressed as $\overrightarrow{OA} = \boldsymbol{x}_1 - \overrightarrow{AT1}$. Thus vector $\overrightarrow{AT2}$ is $\overrightarrow{AT2} = \boldsymbol{x}_2 - \overrightarrow{OA} = \boldsymbol{x}_2 - \boldsymbol{x}_1 + \overrightarrow{AT1}$. If the angle $\beta$ $(0 \leq \beta \leq \pi)$ between the vectors $\overrightarrow{AT2}$ and $\overrightarrow{AT1}$ is greater than $\alpha$, $T2$ is not inside the cone;

$$\beta = \cos^{-1}\left(\frac{(\overrightarrow{AT2})'\overrightarrow{AT1}}{L_{\overrightarrow{AT2}}L_{\overrightarrow{AT1}}}\right) \qquad (10)$$

Substituting $\overrightarrow{AT1} = (R/\kappa \cos\theta, \ R/\kappa \sin\theta)$, $\overrightarrow{AT2} = (x_2 - x_1 + (R/\kappa)\cos\theta, y_2 - y_1 + (R/\kappa)\sin\theta)$ into equation (10), $\beta$ can be written as the function of $R, \kappa, \theta$ and the turbines' positions $\boldsymbol{x}_1$ and $\boldsymbol{x}_2$.

Let

$$\beta_{i,j} = \beta_{i,j}\left(\theta, x_i, y_i, x_j, y_j\right) \qquad (11)$$

be the angle used to determine whether turbine $i$ is in the cone of turbine $j$ given the wind direction $\theta$.

**Lemma 2**. If wind turbine $i$ is inside the wake of turbine $j$, $d_{i,j}$ is the distance between turbine $i$ and $j$ projected on the wind direction $\theta$, $d_{i,j} = |(x_i - x_j)\cos\theta + (y_i - y_j)\sin\theta|$.

Proof:

The vector $\overrightarrow{T1T2}$ from $T1$ to $T2$ is calculated as $\boldsymbol{x}_2 - \boldsymbol{x}_1$; thus the projection length of $\overrightarrow{T1T2}$ on $\overrightarrow{AT1}$ is    Thus $d_{i,j}$ can be written as

$$\frac{|\overrightarrow{T1T2}'\overrightarrow{AT1}|}{L_{\overrightarrow{AT1}}} = \kappa \frac{|(x_2 - x_1)\left(\frac{R}{\kappa}\cos\theta\right) + (y_2 - y_1)\left(\frac{R}{\kappa}\sin\theta\right)|}{R} = |(x_2 - x_1)\cos\theta + (y_2 - y_1)\sin\theta| \qquad (12)$$
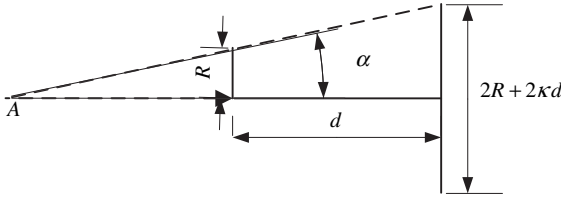
Fig. 3. An imaginary half cone of a wind turbine.

$$d_{i,j} = \left| (x_i - x_j)\cos\theta + (y_i - y_j)\sin\theta \right| \tag{13}$$

and equation (8) can be rewritten as

$$Vel\_def_i = \sqrt{\sum_{j=1,\, j\neq i,\, \beta_{i,j}<\alpha}^{N} Vel\_def_{i,j}^2} \tag{14}$$

It is easy to observe that $Vel\_def_i$ is a function of $\theta$ and all turbine locations. It is shown that only scaling parameter $c$ of a Weibull distribution will be affected by the wake loss [6], i.e.,

$$c_i(\theta) = c(\theta) \times (1 - Vel\_def_i), \quad i = 1, \dots, N \tag{15}$$

Thus equation (16) stands for the expected power production of a single turbine.

$$E(P_i) = \int_0^{360} p_\theta(\theta) E(P_i, \theta)\mathrm{d}\theta = \int_0^{360} p_\theta(\theta)\mathrm{d}\theta$$
$$\times \int_0^\infty f(v)\frac{k(\theta)}{c_i(\theta)}\left(\frac{v}{c_i(\theta)}\right)^{k(\theta)-1} e^{-(v/c_i(\theta))^{k(\theta)}}\mathrm{d}v \tag{16}$$

Although the wake loss model considered in this paper is rather simple, other complex wake loss models [3,7] can be incorporated into the proposed optimization approach. Once the wake loss can be calculated based on wind turbine locations, the power curve function needs be determined for estimation of the expected power production.

## 3. Power curve

Though a power curve $P = f(v)$ usually resembles a sigmoid function, it could be described as a linear function with a tolerable error. For example, model (17) illustrates a linear power curve function, where $v_{\text{cut}-\text{in}}$ is the cut-in wind speed. If the wind speed is smaller than the cut-in speed, there is no power output because the torque is not sufficient enough to turn the generator. Similarly, if the wind speed is greater than the rated speed and smaller than the cut-out speed $v_{\text{cut}-\text{out}}$, the wind turbine control system will keep the power output stable (fixed at $P_{\text{rated}}$) to protect the system from hazardous loads. When the wind speed is between the cut-in and rated speed, the power output follows a linear equation, where $\lambda$ is the slope parameter, and $\eta$ is the intercept parameter. In future research, the linear power curve function could be replaced by a more accurate nonlinear approximation.

$$f(v) = \begin{cases} 0, & v < v_{\text{cut}-\text{in}} \\ \lambda v + \eta, & v_{\text{cut}-\text{in}} \leq v \leq v_{\text{rated}} \\ P_{\text{rated}}, & v_{\text{cut}-\text{out}} > v > v_{\text{rated}} \end{cases} \tag{17}$$

Using the linear power curve function of equation (17) in equation (16), $\int_0^\infty f(v)\,(k(\theta)/c_i(\theta))\,(v/c_i(\theta))^{k(\theta)-1} e^{-(v/c_i(\theta))^{k(\theta)}}\mathrm{d}v$ breaks into three parts: $\lambda \int_{v_{\text{cut}\_\text{in}}}^{v_{\text{rated}}} v(k(\theta)/c_i(\theta))\,(v/c_i(\theta))^{k(\theta)-1} e^{-(v/c_i(\theta))^{k(\theta)}}\mathrm{d}v$, $\eta \int_{v_{\text{cut}\_\text{in}}}^{v_{\text{rated}}} (k(\theta)/c_i(\theta))\,(v/c_i(\theta))^{k(\theta)-1} e^{-(v/c_i(\theta))^{k(\theta)}}\mathrm{d}v$ and $P_{\text{rated}} \int_{v_{\text{rated}}}^\infty (k(\theta)/c_i(\theta))\,(v/c_i(\theta))^{k(\theta)-1} e^{-(v/c_i(\theta))^{k(\theta)}}\mathrm{d}v$ which can be simplified further.

$P_{\text{rated}} \int_{v_{\text{rated}}}^\infty (k(\theta)/c_i(\theta))\,(v/c_i(\theta))^{k(\theta)-1} e^{-(v/c_i(\theta))^{k(\theta)}}\mathrm{d}v$ can be written as $P_{\text{rated}}(1 - \Pr(v \leq v_{\text{rated}}))$, which is equal to $P_{\text{rated}}\, e^{-(v_{\text{rated}}/c_i(\theta))^{k(\theta)}}$. $\eta \int_{v_{\text{cut}\_\text{in}}}^{v_{\text{rated}}} (k(\theta)/c_i(\theta))\,(v/c_i(\theta))^{k(\theta)-1} e^{-(v/c_i(\theta))^{k(\theta)}}\mathrm{d}v$ can be written as $\eta(e^{-(v_{\text{cut}-\text{in}}/c_i(\theta))^{k(\theta)}} - e^{-(v_{\text{rated}}/c_i(\theta))^{k(\theta)}})$.

It is difficult to obtain an analytical form of the expression $\int_{v_{\text{cut}\_\text{in}}}^{v_{\text{rated}}} v(k(\theta)/c_i(\theta))\,(v/c_i(\theta))^{k(\theta)-1} e^{-(v/c_i(\theta))^{k(\theta)}}\mathrm{d}v = \int_{v_{\text{cut}\_\text{in}}}^{v_{\text{rated}}} v\,d(1 - e^{-(v/c_i(\theta))^{k(\theta)}})$.
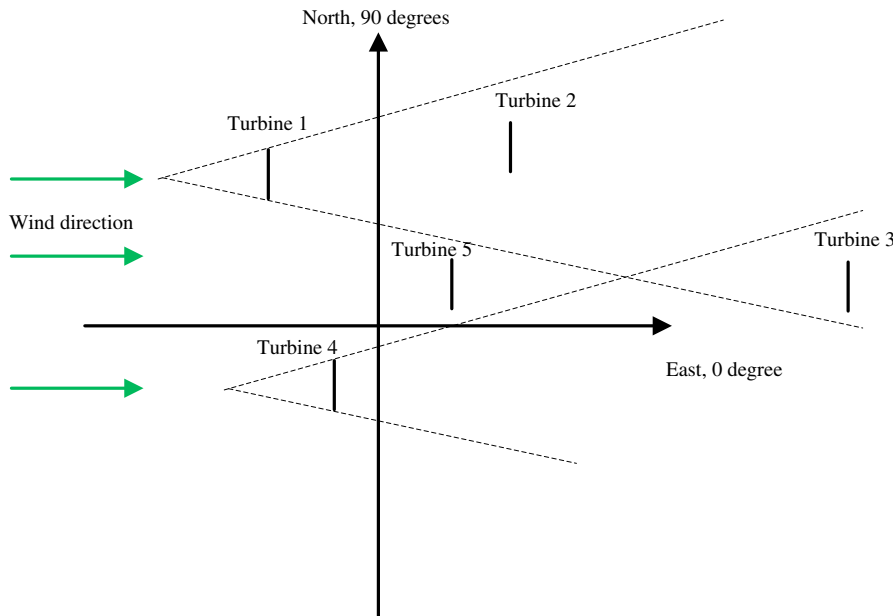


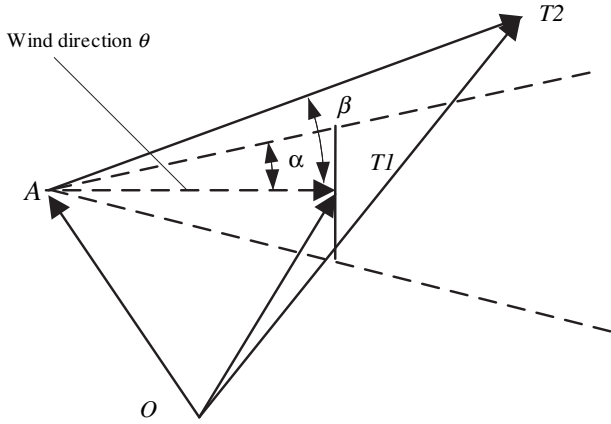Fig. 4. Turbines affected by the wake of other turbines.

Fig. 5. A wind turbine inside the cone of another turbine.

However, if the wind speed is discretized into small bins, the integration can be approximated with the Riemann sum [11]. Later in the paper, the wind speed and its direction are discretized so that numerical integration can be performed. It needs to be noted that continuous wind characteristics are not available in the design of wind farms.

## 4. Discretization of wind speed and wind direction

Assume the wind direction is discretized into $N_\theta + 1$ bins of equal width; let $\theta_1, \theta_2, ..., \theta_{N_\theta}$ be the dividing points of wind direction with $0° < \theta_1 \leq \theta_2 \leq ... \leq \theta_{N_\theta} < 360°$, $\theta_0 = 0°$, $\theta_{N_\theta+1} = 360°$. Each bin is associated with a relative frequency $0 \leq \omega_i \leq 1$, $i = 0, ..., N_\theta$. For example $\omega_0$ is the frequency of bin $[0°, \theta_1]$, $\omega_{N_\theta}$ is the frequency of bin $[\theta_{N_\theta}, 360°]$. The frequency $\omega_i$ can be easily estimated from the wind data.

Wind speed is also discretized into $N_v + 1$ bins; let $v_1, v_2, v_3, ..., v_{N_v}$ be the dividing points of wind speed with $v_{cut-in} < v_1 \leq v_2 \leq v_3 \leq ... \leq v_{N_v} < v_{rated}$, $v_0 = v_{cut-in}$, $v_{N_v+1} = v_{rated}$.
$\int_{v_{cut\_in}}^{v_{rated}} v(k(\theta)/c_i(\theta)) (v/c_i(\theta))^{k(\theta)-1} e^{-(v/c_i(\theta))^{k(\theta)}} dv$ can be approximated as $\sum_{j=1}^{N_v+1} \{e^{-(v_{j-1}/c_i(\theta))^{k(\theta)}} - e^{-(v_j/c_i(\theta))^{k(\theta)}}\}((v_{j-1}+v_j)/2)$, so $E(P_i) = \int_0^{360} p_\theta(\theta) (\lambda \sum_{j=1}^{N_v+1} \{(e^{-(v_{j-1}/c_i(\theta))^{k(\theta)}} - e^{-(v_j/c_i(\theta))^{k(\theta)}} v_j)_1 + v_j 2)\} + P_{rated} \times e^{-(v_{rated}/c_i(\theta))^{k(\theta)}}) d\theta + \int_0^{360} p_\theta(\theta) \eta (e^{-(v_{cut-in}/c_i(\theta))^{k(\theta)}} - e^{-(v_{rated}/c_i(\theta))^{k(\theta)}}) d\theta$.

For further simplification,

$$E(P_i) = \lambda \sum_{j=1}^{N_v+1} \left(\frac{v_{j-1} + v_j}{2}\right) \int_0^{360} p_\theta(\theta) \left\{ e^{-(v_{j-1}/c_i(\theta))^{k(\theta)}} \right.$$
$$\left. - e^{-(v_j/c_i(\theta))^{k(\theta)}} \right\} d\theta + P_{rated} \int_0^{360} p_\theta(\theta) e^{-(v_{rated}/c_i(\theta))^{k(\theta)}} d\theta$$
$$+ \eta \int_0^{360} p_\theta(\theta) \left( e^{-(v_{cut-in}/c_i(\theta))^{k(\theta)}} - e^{-(v_{rated}/c_i(\theta))^{k(\theta)}} \right) d\theta$$

$P_{rated} \int_0^{360} p_\theta(\theta) e^{-(v_{rated}/c_i(\theta))^{k(\theta)}} d\theta$ can be approximated as $P_{rated} \sum_{l=1}^{N_\theta+1} \{(\theta_l - \theta_{l-1}) p_\theta((\theta_l + \theta_{l-1})/2) e^{-(v_{rated}/c_i(\theta_l+\theta_{l-1}/2))^{k((\theta_l+\theta_{l-1})/2)}}\}$, where $p_\theta((\theta_l + \theta_{l-1})/2)$ can be approximated as $\omega_{l-1}$, which results in $P_{rated} \sum_{l=1}^{N_\theta+1} \{(\theta_l - \theta_{l-1}) \omega_{l-1} e^{-(v_{rated}/c_i((\theta_l+\theta_{l-1})/2))^{k((\theta_l+\theta_{l-1})/2)}}\}$.

Similarly

$\int_0^{360} p_\theta(\theta) \{ e^{-(v_{j-1}/c_i(\theta))^{k(\theta)}} - e^{-(v_j/c_i(\theta))^{k(\theta)}}\} d\theta$ can be calculated as

$$\sum_{l=1}^{N_\theta+1} \left\{ (\theta_l - \theta_{l-1}) \omega_{l-1} \left\{ e^{-(v_{j-1}/c_i((\theta_l+\theta_{l-1})/2))^{k((\theta_l+\theta_{l-1})/2)}} \right. \right.$$
$$\left. \left. - e^{-(v_j/c_i((\theta_l+\theta_{l-1})/2))^{k((\theta_l+\theta_{l-1})/2)}} \right\} \right\}.$$

Similarly $\eta \int_0^{360} p_\theta(\theta) (e^{-(v_{cut-in}/c_i(\theta))^{k(\theta)}} - e^{-(v_{rated}/c_i(\theta))^{k(\theta)}}) d\theta$ can be calculated as

$$\eta \sum_{l=1}^{N_\theta+1} \left\{ (\theta_l - \theta_{l-1}) \omega_{l-1} \left( e^{-\left(v_{cut-in}/c_i\left(\frac{\theta_l+\theta_{l-1}}{2}\right)\right)^{k\left(\frac{\theta_l+\theta_{l-1}}{2}\right)}} \right. \right.$$
$$\left. \left. - e^{-\left(v_{rated}/c_i\left(\frac{\theta_l+\theta_{l-1}}{2}\right)\right)^{k\left(\frac{\theta_l+\theta_{l-1}}{2}\right)}} \right) \right\}$$

Therefore

$$E(P)_i = \lambda \sum_{j=1}^{N_v+1} \left(\frac{v_{j-1}+v_j}{2}\right) \sum_{l=1}^{N_\theta+1} \left\{ (\theta_l - \theta_{l-1})\omega_{l-1} \right.$$
$$\left\{ e^{-\left(v_{j-1}/c_i\left(\frac{\theta_l+\theta_{l-1}}{2}\right)\right)^{k\left(\frac{\theta_l+\theta_{l-1}}{2}\right)}} - e^{-\left(v_j/c_i\left(\frac{\theta_l+\theta_{l-1}}{2}\right)\right)^{k\left(\frac{\theta_l+\theta_{l-1}}{2}\right)}} \right\} \right\}$$
$$+ P_{rated} \sum_{l=1}^{N_\theta+1} \left\{ (\theta_l - \theta_{l-1})\omega_{l-1} e^{-\left(v_{rated}/c_i\left(\frac{\theta_l+\theta_{l-1}}{2}\right)\right)^{k\left(\frac{\theta_l+\theta_{l-1}}{2}\right)}} \right\}$$
$$+ \eta \sum_{l=1}^{N_\theta+1} \left\{ (\theta_l - \theta_{l-1})\omega_{l-1} \left( e^{-\left(v_{cut-in}/c_i\left(\frac{\theta_l+\theta_{l-1}}{2}\right)\right)^{k\left(\frac{\theta_l+\theta_{l-1}}{2}\right)}} \right. \right.$$
$$\left. \left. - e^{-\left(v_{rated}/c_i\left(\frac{\theta_l+\theta_{l-1}}{2}\right)\right)^{k\left(\frac{\theta_l+\theta_{l-1}}{2}\right)}} \right) \right\} \quad (18)$$

Substituting equation (18) into model (4) makes it is easy to solve the resultant optimization model. Once wind speed and wind direction are discretized into small bins, $c_i(.)$ and $k(.)$ can estimated from the historical wind data. Discretization makes the calculation of the expected power tractable. Though model (4) is a constrained nonlinear optimization problem, considering nonlinear power curves or more complex wake loss models, and additional constraints would increase its complexity. Thus selecting a flexible optimization algorithm is important. This model complexity warrants the use of a population based search algorithm, such as the evolutionary strategy algorithm.

## 5. Evolutionary strategy algorithm

The solution of model (4) can be encoded as a vector used by an evolutionary strategy algorithm [14].

The general form of the $j$th individual in the evolutionary strategy algorithm is defined as $(\mathbf{z}^j, \boldsymbol{\sigma}^j)$, where $\mathbf{z}^j$ and $\boldsymbol{\sigma}^j$ are two vectors with $2N$ entries, i.e., $\mathbf{z}^j = (x_1^j, y_1^j, ..., x_N^j, y_N^j)^T$, $\boldsymbol{\sigma}^j = (\sigma_{1,x}^j, \sigma_{1,y}^j, ..., \sigma_{N,x}^j, \sigma_{N,y}^j)^T$.

The pair $(x_1^j, y_1^j)$ is the position of the first turbine, while $(\sigma_{1,x}^j, \sigma_{1,y}^j)$ is used to mutate the first turbine's position. The pair $(x_N^j, y_N^j)$ is the position of the $N$th turbine and $(\sigma_{N,x}^j, \sigma_{N,y}^j)$ is used to mutate the $N$th turbine's position.

Each element of $\boldsymbol{\sigma}^j$ is used as a standard deviation of a normal distribution with zero mean. $\boldsymbol{\sigma}^j$ is used to mutate the solution $\mathbf{z}^j$.

The initial population $\boldsymbol{\sigma}^j$ $(j = 1, ..., \mu_{Child})$ is generated by uniformly sampling from the range $[\boldsymbol{\sigma}_{low}, \boldsymbol{\sigma}_{up}]$, where $\boldsymbol{\sigma}_{low}$ and $\boldsymbol{\sigma}_{up}$ are the lower and upper bounds for the standard deviation vector.

In this paper, a multi-objective evolutionary algorithm is used as a basic algorithm to solve a constrained optimization problem [2].

All the constraints are transformed to formulate the second objective function. To standardize the optimization problem, model (4) is transformed into a minimization problem with two objectives.

$$\min\{Obj_1, Obj_2\}$$

where $Obj_1 = 1/\sum_{i=1}^{N} E(P_i))$ and

$$Obj_2 = \sum_{i=1}^{N} \max\{0, x_i^2 + y_i^2 - r^2\}$$

$$+ \sum_{i=1}^{N} \sum_{j=1, j\neq i}^{N} \max\left\{0, 64R^2 - (x_i - x_j)^2 - (y_i - y_j)^2\right\}.$$

Minimizing $Obj_1$ equals maximizing the expected energy output. The minimum of $Obj_2$ is zero, which means all constraints are satisfied. To solve the double-objective optimization problem, an evolutionary strategy algorithm, SPEA [14], is used. This algorithm matches the complexity of the underlying problem.

### 5.1. The algorithm

1 Initialize three empty sets *Parent*, *Offspring* and *Elite*. Randomly generate $\mu_{Child}$ individuals (solutions) to form the initial children population and place them in *Offspring*.
2 Repeat until the stopping criterion is satisfied.
2.1 Find non-dominated solutions in *Offspring* and copy them into *Elite*. Remove dominated solutions in *Elite*. Reduce the size of *Elite* by clustering, if necessary.
2.2 Fitness assignment: Assign fitness to individuals in *Offspring* and *Elite*.
2.3 Selection: use tournament selection to select $\mu_{Parent}$ individuals from *Offspring* ⊔ *Elite* and store them in *Parent*.
2.4 Recombination: Generate a new population *Offspring* by selecting two parents in *Parent*.
2.5 Mutation: Mutate the individuals in *Offspring*.
2.6 Assign fitness to the individuals in *Offspring*.

The stopping criterion in this paper is the number of generations.

### 5.2. Mutation

An individual $(z^j, \sigma^j)$ can be mutated by following the equations (19) and (20), with $\sigma^j$ mutated first, $z^j$ mutated next.

$$\sigma^j = \sigma^j \cdot \left(e^{N(0,\tau')+N_{1,x}(0,\tau)}, e^{N(0,\tau')+N_{1,y}(0,\tau)}, \ldots e^{N(0,\tau')+N_{N,x}(0,\tau)},\right.$$

$$\left. e^{N(0,\tau')+N_{N,y}(0,\tau)}\right) \tag{19}$$

where $N(0, \tau')$ is a random number drawn from normal distribution with 0 mean and standard deviation $\tau'$; $N_{i,x}(0,\tau)$ and $N_{i,y}(0,\tau)$ ($i = 1\ldots N$) are two random numbers drawn from normal distribution with a mean of 0 and standard deviation $\tau$; $N_{i,x}(0,\tau)$ is generated specifically for $\sigma_{i,x}^i$; $N_{i,y}(0,\tau)$ is generated specifically for $\sigma_{i,y}^i$, while $N(0,\tau')$ is for all entries; and "·" denotes the Hadamard matrix product [16].

The new solution is generated from equation (20).

$$z^j = z^j + N\left(\mathbf{0}, \sigma^j\right) \tag{20}$$

where $N(\mathbf{0}, \sigma^j)$ is a vector of the same size as $z^j$. Each element of $N(\mathbf{0}, \sigma^j)$ is generated from a normal distribution with a mean of 0 and the corresponding standard deviation in vector $\sigma^j$.

### 5.3. Selection and recombination of parents

To generate $\mu_{Child}$ children, two parents are selected from the parent population and recombined $\mu_{Child}$ times. Assume each time two parents are selected randomly to produce one child by using equation (21):

$$\left(\frac{\sum_{j\in SelectedParents} z^j}{2}, \frac{\sum_{j\in SelectedParents} \sigma^j}{2}\right) \tag{21}$$

*SelectedParents* is a set consisting of the two indices of the randomly selected parents.

### 5.4. Tournament selection

Tournament selection [15] with replacement is used in this paper to select out promising individuals going into the next generation based on their fitness values. The tournament size is a predefined parameter to control the selection pressure.

## 6. Computational study

To illustrate the concepts presented in this paper, numerical examples and an industrial case study are presented. The wind turbines used in this paper have the following parameters: rotor radius is 38.5 (m); cut-in speed is 3.5 (m/s); rated speed is 14 (m/s); rated power is 1500 (kW). For the linear power curve function, $\lambda = 140.86$, $\eta = -500$. Hub height is 80 (m). The thrust coefficient $C_T$ is assumed to be 0.8, the spreading constant $\kappa$ is assumed to be 0.075 for land cases.

Knowing the cut-in wind speed and the rated wind speed, wind speed is divided at $N_v = 20$ intervals of 0.5 (m) each. Similarly, the wind direction is divided at $N_\theta = 23$ intervals of 15° each.

Some of the parameters of the evolutionary algorithm used in this paper are fixed throughout all experiments. The tournament size is fixed at 4. Initial population $z^j$ is generated by uniformly sampling from $[-r, r]$. During the optimization process, all solutions are checked for non-violation of the interval constraint. Similarly $\sigma^j$ is limited to $[\sigma_{low}, \sigma_{up}]$ set at $[1, r/20]$. In other words, the minimum standard deviation for mutating the solution is set at 1 (m); the maximum standard deviation is heuristically set at 1/20 of the farm radius, and it increases with the farm radius. Based on the heuristic knowledge [15], $\tau'$ is calculated as $\tau' = 1/\sqrt{4N}$, $\tau$ is calculated as $\tau = 1/\sqrt{2\sqrt{2N}}$. The number of generations in this paper is set to 100.

**Table 1**
Wind scenario 1.

| $l-1$ | $\theta_{l-1}$ | $\theta_l$ | $k$ | $c$ | $\omega_{l-1}$ | $l-1$ | $\theta_{l-1}$ | $\theta_l$ | $k$ | $c$ | $\omega_{l-1}$ |
|---|---|---|---|---|---|---|---|---|---|---|---|
| 0 | 0 | 15 | 2 | 13 | 0 | 12 | 180 | 195 | 2 | 13 | 0.01 |
| 1 | 15 | 30 | 2 | 13 | 0.01 | 13 | 195 | 210 | 2 | 13 | 0.01 |
| 2 | 30 | 45 | 2 | 13 | 0.01 | 14 | 210 | 225 | 2 | 13 | 0.01 |
| 3 | 45 | 60 | 2 | 13 | 0.01 | 15 | 225 | 240 | 2 | 13 | 0.01 |
| 4 | 60 | 75 | 2 | 13 | 0.01 | 16 | 240 | 255 | 2 | 13 | 0.01 |
| 5 | 75 | 90 | 2 | 13 | 0.2 | 17 | 255 | 270 | 2 | 13 | 0.01 |
| 6 | 90 | 105 | 2 | 13 | 0.6 | 18 | 270 | 285 | 2 | 13 | 0.01 |
| 7 | 105 | 120 | 2 | 13 | 0.01 | 19 | 285 | 300 | 2 | 13 | 0.01 |
| 8 | 120 | 135 | 2 | 13 | 0.01 | 20 | 300 | 315 | 2 | 13 | 0.01 |
| 9 | 135 | 150 | 2 | 13 | 0.01 | 21 | 315 | 330 | 2 | 13 | 0.01 |
| 10 | 150 | 165 | 2 | 13 | 0.01 | 22 | 330 | 345 | 2 | 13 | 0.01 |
| 11 | 165 | 180 | 2 | 13 | 0.01 | 23 | 345 | 360 | 2 | 13 | 0 |
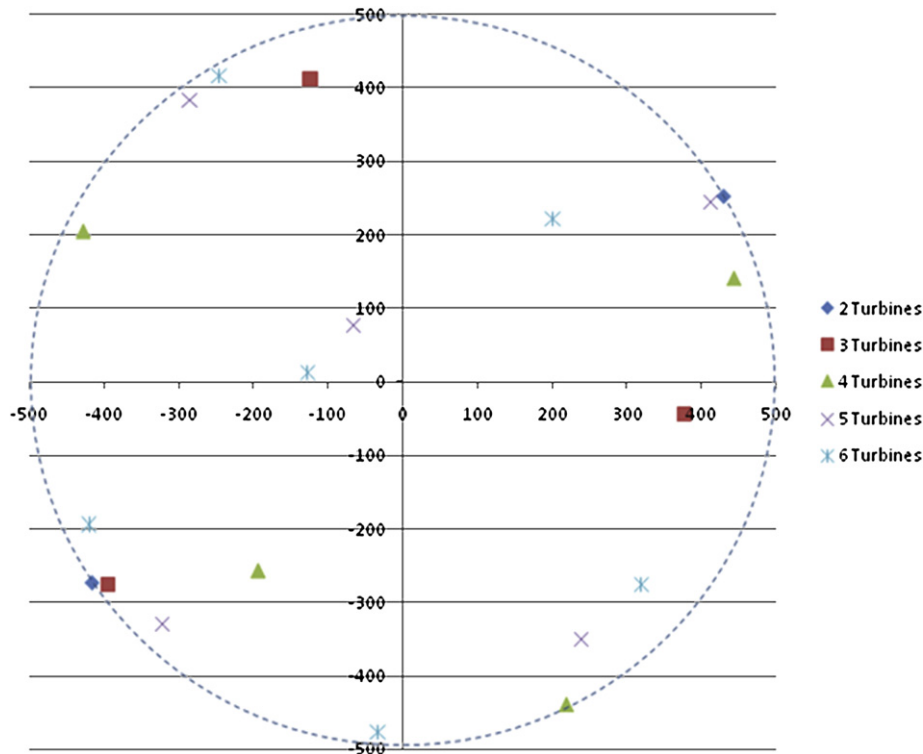
**Fig. 6.** Layout solutions for different number of turbines given the wind characteristics in Table 1.

### 6.1. Wind scenario 1

The illustrative example used in this paper assumes that the farm radius $r = 500$ (m); the wind characteristic of this example is described in Table 1, which was obtained from analyzing historical wind data. The data in Table 1 can be read as follows: when wind direction is between 0° and 15°, the wind speed follows a Weibull distribution with $k = 2$, $c = 13$; the probability for wind blowing between 0° and 15° is zero. Similarly, when wind direction is between 90° and 105°, the wind speed follows a Weibull distribution with $k = 2$, $c = 13$; the probability for wind blowing between 90° and 105° is 0.6. Table 1 shows that wind blows predominantly from 75° to 105° with a probability of 0.8.

To illustrate the algorithm's ability to optimize the wind farm layout, different numbers of turbines (2–6 turbines) are considered. Fig. 6 shows the optimal layout solutions for different numbers of turbines. The optimal solutions are obtained through $\mu_{Parent}/\mu_{Child} = 20/120$, for 100 generations. During the optimization process, the *Elite* set size is limited to 50. When there are more than 50 individuals in the *Elite* set, a clustering procedure is activated to delete individuals with the same objective function values or similar geometric positions.

Based on Fig. 6, for two turbines to be placed within the farm radius, the algorithm places the two turbines on the boundary of the circle. The line connecting the two turbines appears to be perpendicular to the major wind direction (90°–105°). When there are three turbines to be placed, the algorithm positions the two turbines (lower part of Fig. 6) across the major wind direction, and attempts to locate the third turbine as far as possible from the other two turbines, and to keep it from the wakes of the other two turbines given the major wind direction.

As shown in Fig. 6, when there are 4, 5 or 6 turbines to be located, the algorithm selects the locations, avoiding the wake losses under the major wind directions.

Fig. 7 shows the initial population and the population at the 100th generation for the 6 turbines. It is easy to see that the algorithm converges as the number of generations increases. However, 100 generations are enough to converge for the data used in this example.
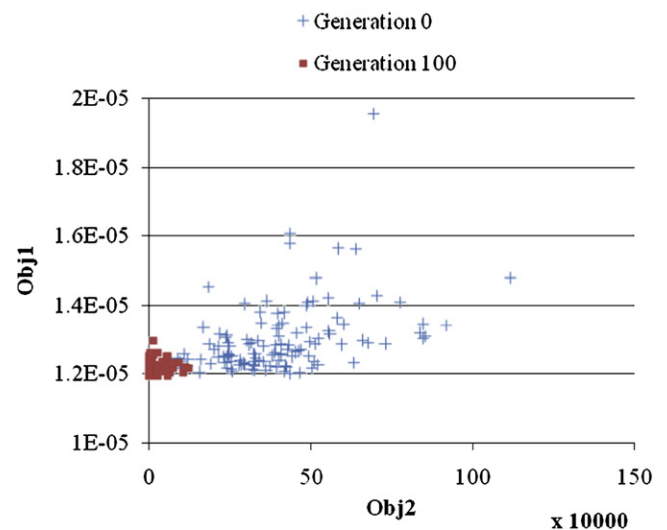


**Fig. 7.** Initial population and the population at the 100th generation.

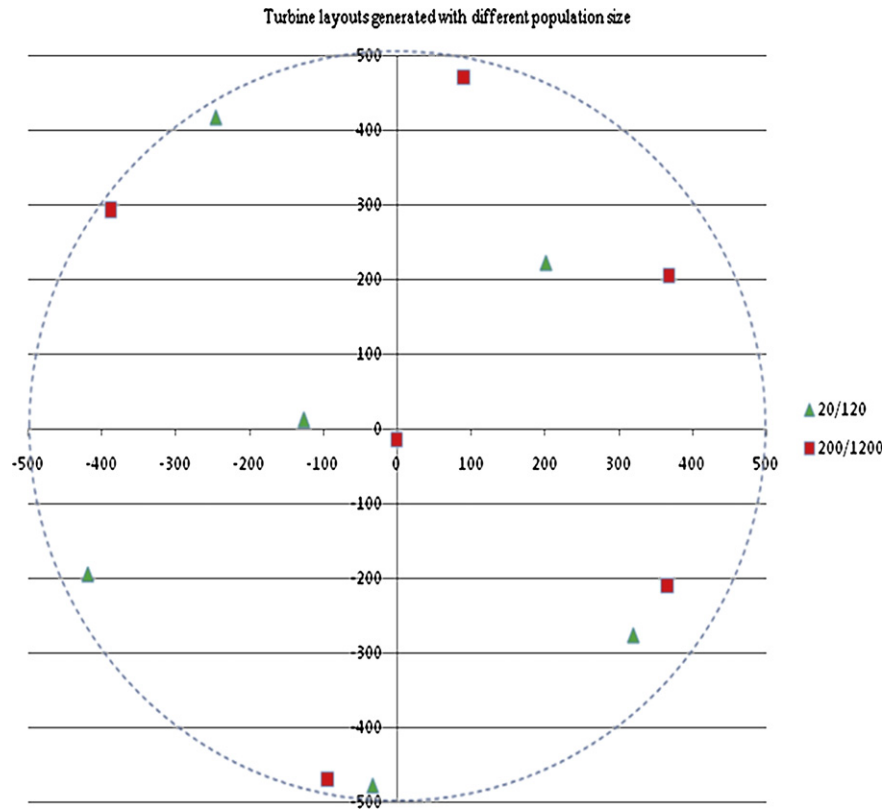Turbine layouts generated with different population size



▲ 20/120
■ 200/1200

**Fig. 8.** Six layouts of turbines generated by using another initial population size.

For a large number of turbines, the search space expands due the increased number of individuals in the ES algorithm. Thus increasing the initial population size seems to be a viable way to search for optimal solutions. Fig. 8 shows two optimal solutions generated with different population sizes. The triangle shapes indicate the locations generated when $\mu_{Parent}/\mu_{Child} = 20/120$. The square shapes show the locations generated when $\mu_{Parent}/\mu_{Child} = 200/1200$. Using $\mu_{Parent}/\mu_{Child} = 20/120$, the algorithm can find $Obj_1 = 1.1939 \times 10^{-5}$. Using $\mu_{Parent}/\mu_{Child} = 200/1200$, the algorithm finds $Obj_1 = 1.1937 \times 10^{-5}$, which is a better value than in the case of a smaller initial population.

Note that increasing the population size leads to better quality solutions. It is worth mentioning that the tournament size should also be modified when the population size changes.

### 6.2. Wind scenario 2

Table 2 shows the wind data collected from an industrial wind farm. For this wind farm, the wind blows predominantly from 120° to 225°, which is a wider direction spectrum than that of wind scenario 1. Wind scenario 1 is easier to see whether the optimization results make sense in terms of minimizing wake loss.

Fig. 9 shows the optimal layout solutions for different numbers of turbines (2–6). In this wind scenario 2, wind farm radius is still assumed to be 500 (m). All the solutions are generated with $\mu_{Parent}/\mu_{Child} = 20/120$, for 100 generations. The line connecting the two turbines pretends to be perpendicular to the major wind direction (120°–225°). When there are three turbines to be placed, the algorithm positions the two turbines across the major wind direction, and attempts to locate the third turbine as far as possible from the other two turbines,

while minimizing the wake loss generated by the third turbine from the major wind directions. As in Fig. 9, when there are 4, 5 or 6 turbines to be located, the algorithm selects the locations, avoiding the wake losses under the major wind directions.

Note that when the wind direction displays a wide range, it is almost impossible for human heuristics to derive an optimal solution. In this case, a wind farm layout optimization tool is necessary for designing turbine locations.

### 6.3. Wake loss

If it is assumed that there is no wake loss, the expected power can be calculated from equation (22) by substituting $c_i(.)$ with $c(.)$ in equation (18). In this scenario, optimal turbine locations only need to satisfy the distance constraints.

**Table 2**
Wind scenario 2.

| $l-1$ | $\theta_{l-1}$ | $\theta_l$ | $k$ | $c$ | $\omega_{l-1}$ | $l-1$ | $\theta_{l-1}$ | $\theta_l$ | $k$ | $c$ | $\omega_{l-1}$ |
|---|---|---|---|---|---|---|---|---|---|---|---|
| 0 | 0 | 15 | 2 | 7 | 0.0002 | 12 | 180 | 195 | 2 | 10 | 0.1839 |
| 1 | 15 | 30 | 2 | 5 | 0.008 | 13 | 195 | 210 | 2 | 8.5 | 0.1115 |
| 2 | 30 | 45 | 2 | 5 | 0.0227 | 14 | 210 | 225 | 2 | 8.5 | 0.0765 |
| 3 | 45 | 60 | 2 | 5 | 0.0242 | 15 | 225 | 240 | 2 | 6.5 | 0.008 |
| 4 | 60 | 75 | 2 | 5 | 0.0225 | 16 | 240 | 255 | 2 | 4.6 | 0.0051 |
| 5 | 75 | 90 | 2 | 4 | 0.0339 | 17 | 255 | 270 | 2 | 2.6 | 0.0019 |
| 6 | 90 | 105 | 2 | 5 | 0.0423 | 18 | 270 | 285 | 2 | 8 | 0.0012 |
| 7 | 105 | 120 | 2 | 6 | 0.029 | 19 | 285 | 300 | 2 | 5 | 0.001 |
| 8 | 120 | 135 | 2 | 7 | 0.0617 | 20 | 300 | 315 | 2 | 6.4 | 0.0017 |
| 9 | 135 | 150 | 2 | 7 | 0.0813 | 21 | 315 | 330 | 2 | 5.2 | 0.0031 |
| 10 | 150 | 165 | 2 | 8 | 0.0994 | 22 | 330 | 345 | 2 | 4.5 | 0.0097 |
| 11 | 165 | 180 | 2 | 9.5 | 0.1394 | 23 | 345 | 360 | 2 | 3.9 | 0.0317 |
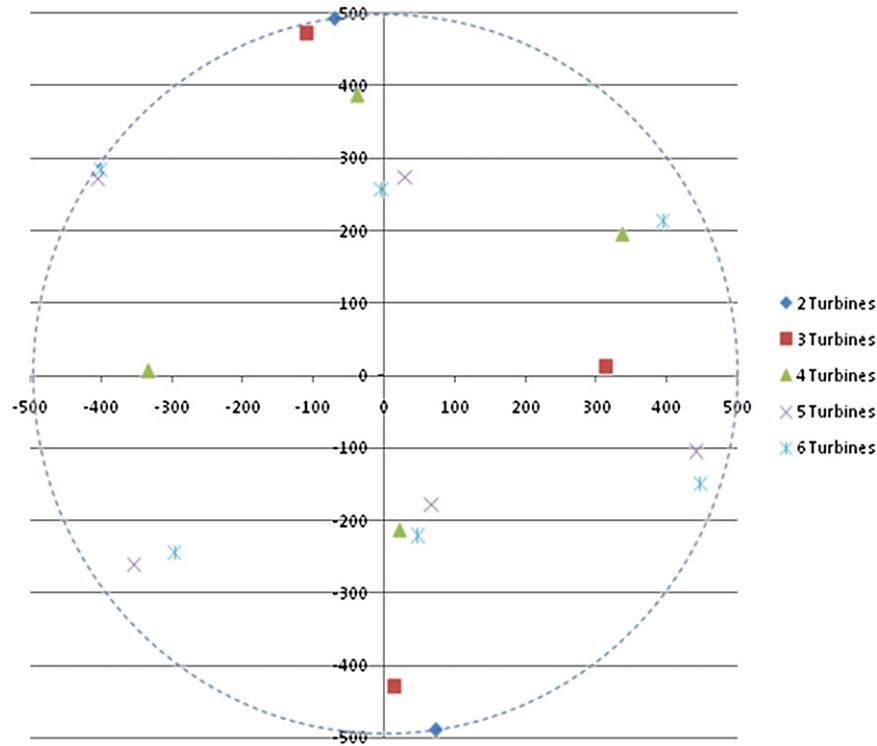
**Fig. 9.** Layout solutions for different numbers of turbines under the wind characteristics in Table 2.

$$
E(P_i) = \lambda \sum_{j=1}^{N_v+1} \left(\frac{v_{j-1}+v_j}{2}\right) \sum_{l=1}^{N_\theta+1} \left\{ (\theta_l - \theta_{l-1})\omega_{l-1} \right.
$$
$$
\times \left\{ e^{-\left(v_{j-1}/c\left(\frac{\theta_l+\theta_{l-1}}{2}\right)\right)^{k\left(\frac{\theta_l+\theta_{l-1}}{2}\right)}} - e^{-\left(v_j/c\left(\frac{\theta_l+\theta_{l-1}}{2}\right)\right)^{k\left(\frac{\theta_l+\theta_{l-1}}{2}\right)}} \right\} \right\}
$$
$$
+ P_{\text{rated}} \sum_{l=1}^{N_\theta+1} \left\{ (\theta_l - \theta_{l-1})\omega_{l-1} e^{-\left(v_{\text{rated}}/c\left(\frac{\theta_l+\theta_{l-1}}{2}\right)\right)^{k\left(\frac{\theta_l+\theta_{l-1}}{2}\right)}} \right\}
$$
$$
+ \eta \sum_{l=1}^{N_\theta+1} \left\{ (\theta_l - \theta_{l-1})\omega_{l-1} \left(e^{-\left(v_{\text{cut-in}}/c\left(\frac{\theta_l+\theta_{l-1}}{2}\right)\right)^{k\left(\frac{\theta_l+\theta_{l-1}}{2}\right)}} \right.\right.
$$
$$
\left.\left. - e^{-\left(v_{\text{rated}}/c\left(\frac{\theta_l+\theta_{l-1}}{2}\right)\right)^{k\left(\frac{\theta_l+\theta_{l-1}}{2}\right)}} \right) \right\} \tag{22}
$$

Thus equation (22) can be regarded as the ideal scenario where the maximum expected energy production from a wind turbine can be achieved. For a given number of turbines, equation (22) can be used to calculate the ideal energy production for a wind farm without considering wake loss.

Once the wake loss is considered, adding additional turbines to the wind farm may cause energy loss. Tables 3 and 4 are generated based on the two different wind scenarios, 1 and 2.

The data in Table 3 is read as: when there are two turbines to be placed in a wind farm, the optimized solution generated by the evolutionary algorithm provides 28083.42 kW of expected energy production (note that the yearly production is not computed). If there is no wake loss, the ideal energy production is 28091.47 kW; the potential wake loss under this layout solution is calculated by using 28091.47 − 28083.42 = 8.05. Tables 3 and 4 show that as the number of turbines increases, the wake loss increases.

Fig. 10 shows that for two different wind scenarios, the wake loss of wind scenario 1 is similar to the wake loss of wind scenario 2 when the number of turbines is 2–5. When the number of turbines is 6, the wake loss of wind scenario 2 is significantly higher than that of wind scenario 1. The reason is obvious, as wind scenario 2 includes a wider range of wind directions with a certain probability. However, in wind scenario 1, the wind direction is limited to 75°–105°; other wind directions have almost zero probability, which makes it easier to place turbines and avoid wake loss.

Based on Fig. 10, for a given wind farm radius, it is obvious that there should be some limit on the number of turbines to be placed on a farm. Locating too many turbines will significantly increase wake loss. Based on the constraints listed in model (4), placing 7 turbines within a wind farm of a 500-m radius is not possible. The

**Table 3**
Optimized vs. ideal energy production and wake loss for different numbers of turbines under wind scenario 1.

| No. of turbines | Optimized (kW) | Ideal (kW) | Wake loss (kW) |
|---|---|---|---|
| 2 | 28083.42 | 28091.47 | 8.05 |
| 3 | 42101.06 | 42137.21 | 36.15 |
| 4 | 56057.77 | 56182.95 | 125.18 |
| 5 | 69922.97 | 70228.69 | 305.72 |
| 6 | 83758.79 | 84274.42 | 515.63 |

**Table 4**
Optimized vs. ideal energy production and wake loss for different numbers of turbines under wind scenario 2.

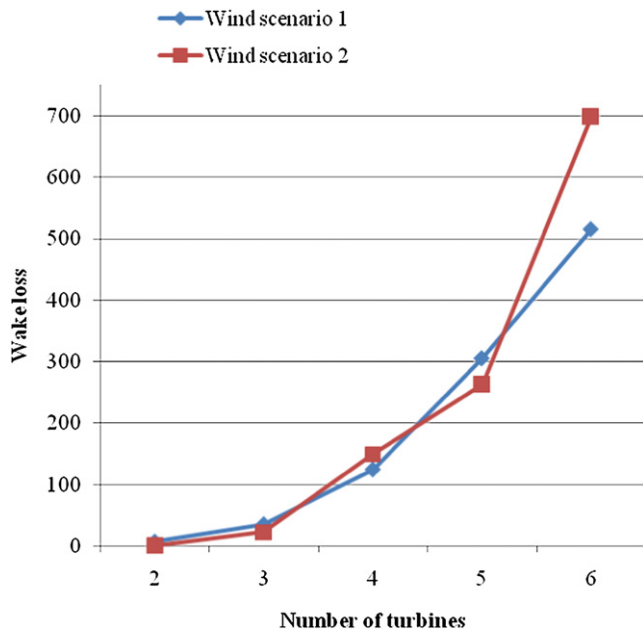| No. of turbines | Optimized (kW) | Ideal (kW) | Wake loss (kW) |
|---|---|---|---|
| 2 | 14631.21 | 14631.37 | 0.16 |
| 3 | 21925.16 | 21947.06 | 21.90 |
| 4 | 29113.71 | 29262.74 | 149.03 |
| 5 | 36316.23 | 36578.43 | 262.20 |
| 6 | 43195.84 | 43894.11 | 698.27 |

**Fig. 10.** Wake loss due to the turbines added to the wind farm.

evolutionary algorithm does not generate a feasible solution when the number of turbines is 7. The minimum distance between two turbines is violated.

## 7. Conclusion

A generic model for optimizing in-land wind farm layout was presented. The optimization model considered wind farm radius and turbine distance constraints. However, other constraints can be easily incorporated in this model. The model maximizes the energy production by placing wind turbines in such a way that the wake loss is minimized.

As the optimization model is nonlinear, and it is hard to derive an analytical solution from the integration part, wind speed and wind direction are discretized into small bins so that the integration can be approximated with discrete summations.

A bi-objective evolutionary strategy algorithm was adopted to solve the constrained nonlinear optimization problem. Both the expected energy production and the constraint violation were optimized. The optimal solution maximized energy production while satisfying all constraints.

Although the wake loss model considered in this paper is a simple one, more complex wake loss models can be considered in the optimization approach discussed in the paper. The complex nonlinear model was solved by the evolutionary strategy algorithm.

Although a global optimal solution is not guaranteed, the quality of the generated solutions is acceptable for industrial applications.

Future research can focus on considering different terrains, e.g., the terrain height information could be incorporated into the model. Furthermore, wind turbine parameter selection could be considered based on the wind farm wind characteristics. For example, for a low wind speed area, there is no need to select large turbines with a high cut-in speed. In other words, it is desirable to maximize the wind turbine capacity utilization factor subject to investment and operational constraints.

## Acknowledgement

## References

[1] AWAE, http://www.awea.org/; 2008.
[2] Cai Z, Wang Y. A multiobjective optimization-based evolutionary algorithm for constrained optimization. IEEE Transactions on Evolutionary Computation 2006;10:658–75.
[3] Crespo A, Hernandez J, Frandsen S. Survey of modeling methods for wind turbine wakes and wind farms. Wind Energy 1999;2:1–24.
[4] Grady SA, Hussaini MY, Abdullah MM. Placement of wind turbines using genetic algorithms. Renewable Energy 2005;30:259–70.
[5] Jensen NO. A note on wind generator interaction. Roskilde, Denmark: Riso National Laboratory; 1983. Technical Report Riso-M-2411.
[6] Lackner MA, Elkinton CN. An analytical framework for offshore wind farm layout optimization. Wind Engineering 2007;31:17–31.
[7] Lange B, Waldl H, Guerrero AG, Heinemann D. Modeling of offshore wind turbine wakes with the wind farm program FLaP. Wind Energy 2003;6: 87–104.
[8] Manwell JF, McGowan JG, Rogers AL. Wind energy explained: theory, design and application. 1st ed. London: John Wiley & Sons; 2002.
[9] Mosetti G, Poloni C, Diviacco B. Optimization of wind turbine positioning in large wind farms by means of a genetic algorithm. Journal of Wind Engineering and Industrial Aerodynamics 1994;51:105–16.
[10] Neustadter HE. Method for evaluating wind turbine wake effects on wind farm performance. Journal of Solar Energy Engineering 1985;107:240–3.
[11] Stroock DW. A concise introduction to the theory of integration. 3rd ed. Birkhauser; 1998.
[12] Walford CA. Wind turbine reliability: understanding and minimizing wind turbine operation and maintenance costs. Available from:. Albuquerque, New Mexico: Sandia National Laboratories www.prod.sandia.gov/cgi-bin/techlib/access-control.pl/2006/061100.pdf; 2006.
[13] Wiser R, Bolinger M. Annual report on U.S. wind power installation, cost, and performance trends: 2006. Available from. Golden, CO: NREL, US Department of Energy, http://www.nrel.gov/wind/pdfs/41435.pdf; 2007.
[14] Zitzler E, Thiele L. Multiobjective evolutionary algorithms: a comparative case study and the strength Pareto approach. IEEE Transactions on Evolutionary Computation 1999;3:257–71.
[15] Eiben AE, Smith JE. Introduction to evolutionary computation. New York: Springer-Verlag; 2003.
[16] Roger H, Charles J. Topics in Matrix Analysis. Cambridge; 1994.
[17] Castro Mora J, Calero Baron JM, Riquelme Santos JM, Burgos Payan M. An evolutive algorithm for wind farm optimal design. Neurocomputing 2007;70:2651–8.
[18] WASP, http://www.wasp.dk/; 2009.